Probing the properties of the 0_2^+ state of ^{4}He via ^{4}He + ^{4}He elastic and exclusive inelastic scattering measurements

V. Soukeras[1,*], *F.* Cappuzzello[1,2], *C.* Agodi[1], *H -W.* Becker[3], *G. A.* Brischetto[1,2], *S.* Calabrese[1], *D.* Carbone[1], *M.* Cavallaro[1], *C.* Ciampi[4], *M.* Cicerchia[5], *M.* Cinausero[5], *I.* Ciraldo[1,2], *D.* Dell'Aquila[6,7], *M.* Fisichella[1], *C.* Frosin[4], *A.* Hacisalihoglu[1,8], *M.* Hilcker[3], *Y.* Kucuk[9], *I.* Lombardo[2], *T.* Marchi[5], *O.* Sgouros[1,2], *A.* Spatafora[1,2], *D.* Torresi[1], *M.* Vigilante[6,7], and *A.* Yildirim[9]

[1]INFN – Laboratori Nazionali del Sud, Catania, Italy
[2]Dipartimento di Fisica e Astronomia "Ettore Majorana", Università di Catania, Catania, Italy
[3]Ruhr-Universitat Bochum, Bochum, Germany
[4]INFN – Sezione di Firenze, Firenze, Italy
[5]INFN – Laboratori Nazionali di Legnaro, Legnaro, Italy
[6]Dipartimento di Fisica "Ettore Pancini", Università degli Studi di Napoli "Federico II", Napoli, Italy
[7]INFN – Sezione di Napoli, Napoli, Italy
[8]Institute of Natural Science, Karadeniz Teknik Universitesi, Trabzon, Turkey
[9]Akdeniz University, Antalya, Turkey

Abstract. The ^{4}He+^{4}He inelastic scattering was experimentally investigated in an exclusive measurement at the MAGNEX facility of INFN - LNS, aiming at characterizing the 0_2^+ resonant state of ^{4}He. Both the ^{4}He+^{4}He→^{4}He+^{4}He*→^{4}He+^{3}H+p and ^{4}He+^{4}He→^{4}He+^{4}He*→^{4}He+^{3}He+n configurations were measured together with an elastic scattering measurement in a wide angular range. In the present article, the experimental setup, the measurement and the data reduction are briefly described, pointing out the significance of an exclusive inelastic scattering measurement to suppress the background originating from other processes.

1 Introduction

Helium is the second most abundant and second lightest element in the observable universe. ^{4}He isotope with a natural abundance larger than 99.99 % was produced during Big Bang Nucleosynthesis while, its production continues in the stars. A part of the ^{4}He found in Earth is fed by the α - decay of the heavy radioactive elements. The binding energy per nucleon for ^{4}He is significantly higher than all nuclides with a similar number of nucleons, making ^{4}He a well bound nucleus. No bound excited states are existing in its level scheme while, both proton and neutron separation thresholds are very high, being S_p = 19.813 MeV and S_n = 20.578 MeV, respectively. Above such thresholds the ^{4}He nucleus may break either in ^{3}H + p or ^{3}He + n, respectively.

A resonant state with $J^\pi = 0^+$, the same spin and parity with the ground state, is lying in an excitation energy just above the proton separation threshold but, below the neutron separation threshold. Although several works have been devoted to experimentally study that resonance by using (e,e') [1–5], (p,p') [6] or (α,α) [7, 8] probes, many of its properties remain unclear [9]. In more details, ab-initio form factor calculations fail to reproduce the results coming from the existing electron scattering data sets, pointing to possible missing physics in the nuclear Hamiltonian [5, 10]. The disagreement was confirmed in a comparison with new electron scattering data recently reported by S. Kegel et al. in Ref. [5]. On the other hand, new calculations reported in Ref. [11] reproduce well the existing electron scattering data although, they use a simplified interaction. Finally, a phenomenological transition density from the experimental data of Ref. [5] was recently reported in Ref. [12].

In the present work, we aim to shed some light in the puzzle of the 0_2^+ state of ^{4}He by performing new high - precision measurements using the (α,α) probe. Beside that, we aim to resolve previous inconsistencies related to the resonance energy and width. The resonance characterization will be guided by a new exclusive measurement with the very good energy and angular resolution, guaranteed by an experimental setup consisted by the large acceptance MAGNEX spectrometer [13] and the OSCAR detection array [14]. The elastic scattering channel, measured under the same experimental conditions, will be considered together with the inelastic scattering channel in a global theoretical interpretation.

The present article aims to describe briefly the strategy of the measurement and the data reduction, pointing out the significance of an exclusive inelastic scattering measurement.

*e-mail: vasileios.soukeras@lns.infn.it

2 Experimental details

Two relevant experiments were carried out at the MAGNEX facility [13] of the Istituto Nazionale di Fisica Nucleare - Laboratori Nazionali del Sud (INFN - LNS). An ^{4}He beam was accelerated by the K800 Superconducting Cyclotron at E_{lab} = 53.0 MeV and impinged on a solid target built by the implantation of ^{4}He atoms on a thin metal foil. The effective thicknesses of the different target components were measured by using the Rutherford backscattering spectrometry (RBS) technique and are presented in table 1. At the same table we present the energy loss of the ^{4}He particles inside the target material and the ratio of the energy loss versus beam energy, demonstrating that the energy loss inside the target ($\sim$ 62 keV for the first experiment and a $\sim$ 23 keV for the second one) is negligible. Finally, the beam current was measured by a Faraday cup mounted 15 cm downstream of the target while, the solid angle of MAGNEX was delimited by four 1 mm thick Tantalum slits located 25 cm downstream of the target.

2.1 The elastic scattering measurement

In the first experiment, dedicated to the elastic scattering measurement, the α-particle ejectiles were detected by the MAGNEX Focal Plane Detector (FPD) [17–19] which consists of a gas-filled tracker followed by a wall of 60 silicon pad detectors. The FPD tracker includes six sections, each one having on the top a proportional wire. The energy loss of the ions inside the gas was measured by each of the proportional wires while, a segmented anode in 223 pads allows for the determination of the horizontal position and angle. On the other hand, the measurement of the electron drift time inside the gas tracker allows for the determination of the vertical position and angle. The residual energy of the ions was measured by the 60 silicon pads detectors, each one covering a 5 x 7 cm^2 area and having a thickness of 1 mm. A complementary measurement of elastic scattering yields was also performed at the second experiment which was dedicated in the inelastic scattering measurement to cross check. In both experiments, a wide angular range $6.5^o \leq \theta_{lab} \leq 45^o$ was spanned in an angular steps of 0.5^o, corresponding to $13^o \leq \theta_{c.m.} \leq 90^o$.

2.2 The exclusive inelastic scattering measurement

In the second experiment, dedicated to the inelastic scattering measurement, we replaced the tantalum foil with an aluminum one, further decreasing the background coming from target materials other than ^{4}He. A complementary measurement using a target with appropriate proportions of Al, O and C was performed to estimate and subtract the remaining background due to reactions on these materials. However, thanks to an exclusive measurement such background yield is small. The inelastically scattered ^{4}He ions were measured in the MAGNEX spectrometer, as described in 2.1, in coincidence with one of the breakup fragments of the second ^{4}He (^{3}H or ^{3}He, respectively) in the OSCAR (hOdoscope of Silicons for Correlations and Analysis of Reactions) telescope [14]. OSCAR is an array consisted by a Single Sided Silicon Strip Detector (SSSSD) 20μm thick providing an energy loss (ΔE) measurement, followed by 16 silicon pads 300 μm thick arranged in a 4x4 mode, providing the residual energy measurement. Protons coming from the inelastic scattering were also measured in OSCAR but, with lower efficiency than the ^{3}H. The strategy and the experimental conditions of the inelastic scattering measurement are tabulated in table 2 while, more details may be found in [15, 16]. It should be noted that, thanks to the exclusive measurement, the possibility to measure at very forward angles in MAGNEX, the large energy and angular acceptance of our detection system and the appropriate selection of the experimental conditions, it was possible to perform an almost background free measurement. The background due to target impurities ranges between 2 and 6 % and it was appropriately determined and subtracted as described above.

3 Data reduction

The particle identification (PID) of the data collected in MAGNEX was performed as described in [15] following the prescription of Ref. [20]. An unambiguous identification of the Z and A of the ions of interest is demonstrated in the Figs 1,2 of Ref. [15]. A software 10^{th} order ray - reconstruction of the non - linear ejectiles trajectories detected in the FPD was performed [21] based on the measured magnetic fields maps [22, 23]. Subsequently, physics quantities such as the kinetic energy, the scattering angle and the excitation energy were precisely determined. The PID in the OSCAR telescope was based on the standard ΔE - E technique. In the quasi-hyperbolic correlations shown in the Fig. 3 of Ref. [15] one may see the excellent discrimination of ^{4}He, ^{3}He, ^{3}H and protons.

Thanks to the coincidence measurement of ^{4}He particles in MAGNEX and ^{3}H (or ^{3}He) in OSCAR, the background due to the aluminum and other target impurities was extremely suppressed. In figure 1 we present for the first time the excitation energy spectrum acquired both in singles and in exclusive mode. The PID conditions of ^{4}He collected at MAGNEX magnetic spectrometer were applied at both spectra while, the PID conditions of ^{3}H collected at OSCAR telescope were applied only at the exclusive spectrum (blue). It should be noted that, without an exclusive measurement, it would be impossible to discriminate the ^{4}He(0_2^+) resonance at $\sim$ 20.3 MeV due to other processes (mainly due to Aluminum target) leading to ^{4}He production, as demonstrated by the spectrum acquired in singles (red). A condition in the ^{3}H significantly suppresses such background events leading to an almost background free measurement of ^{4}He(0_2^+) resonance. A small remnant of background events, presented in Fig. 1 with the green dashed line, was appropriately subtracted as described in the section 2.2.

Special care was also given to the estimation of the detection efficiency. The multipurpose Monte Carlo simulation algorithm MULTIP [24] was used to simulate the energy and angular profiles of the involved reactions and to determine the detection efficiency of the measurement.

Table 1. Thicknesses of the different target components as obtained in RBS measurements are shown in the second and third column of the table [15, 16]. The energy loss of the ^{4}He beam inside the whole target and the energy loss versus beam energy ratio are shown in the last two columns, respectively.

Material	Thickness (atoms/cm^2)	Thickness (μg/cm^2)	Energy-loss (keV)	Energy-loss / Beam energy ratio
experiment I				
^{4}He	3.7x10^{17} ± 2x10^{16}	2.5 ± 0.13	0.4	7.5x10^{-6}
^{181}Ta	3.2x10^{18} ± 3x10^{16}	950 ± 10	60	0.1 %
^{16}O	5.5x10^{17} ± 1.5x10^{16}	14.6 ± 0.4	2	4x10^{-5}
experiment II				
^{4}He	1.9x10^{17} ± 1.5x10^{16}	1.3 ± 0.1	0.2	4x10^{-6}
^{27}Al	4.6x10^{18} ± 4x10^{16}	210 ± 2	23	4x10^{-4}
^{16}O	1.0x10^{17} ± 4x10^{15}	2.7 ± 0.1	0.3	6x10^{-6}
^{12}C	1.2x10^{16} ± 1x10^{15}	0.2 ± 0.02	0.03	6x10^{-7}

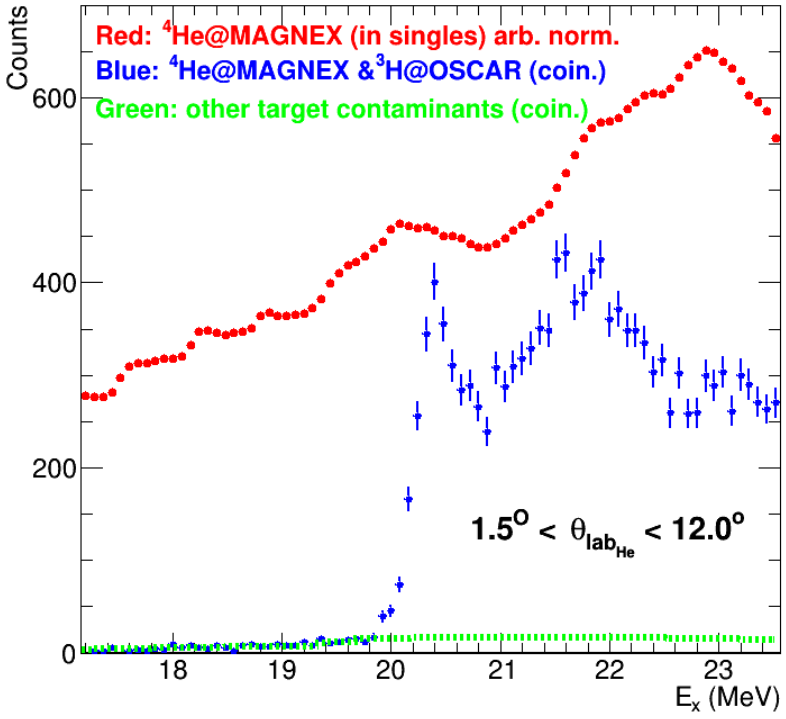

Figure 1. Experimental excitation energy spectrum acquired in singles with PID of ^{4}He ions in MAGNEX spectrometer and the exclusive one with the identified ^{4}He ions in MAGNEX in coincidence with the identified ^{3}H ions in OSCAR telescope are depicted with the red and blue data points, respectively. The spectrum in singles was arbitrarily normalized to guide the eye. The estimation of the background due to other target contaminants was based on a measurement with an ancillary target (see text for details) and is presented with the green dashed line. The spectra refer to the data collected in the complete angular range of both MAGNEX and OSCAR, presented in table 2. Please note that no efficiency correction was applied at the depicted spectra.

The covered angular ranges of the two detection systems in coincidence as well as the selected kinetic energy range in MAGNEX and the detection thresholds in OSCAR were appropriately considered. It should be also noted that since the efficiency may change in different excitation energy and angular regions, an efficiency map was extracted in a small step of dE_x = 0.8 MeV and $d\theta_{lab}$ = 0.5^o interpolating the intermediate regions by using smooth functions. An additional geometrical efficiency related to the "dead regions" of the E - stage of the OSCAR telescope [14] was also taken into account in the determination of the cross section.

The data analysis towards the ^{4}He(0^+_2) characterization is in progress in two directions:

- the line shape analysis which includes the description of the asymmetric line shape of the ^{4}He(0^+_2) resonance and the investigation of the interference phenomena between the resonant and the non - resonant continuum.

Table 2. The strategy and the experimental conditions of the second experiment performed at INFN - LNS, dedicated to inelastic scattering measurement.

Reactions under study	
^{4}He+^{4}He→^{4}He+^{4}He*→^{4}He+^{3}H+p	
^{4}He+^{4}He→^{4}He+^{4}He*→^{4}He+^{3}He+n	
Measurement mode	coincidence
Heavy particle detected	^{4}He in MAGNEX
Light particle detected	^{3}H and ^{3}He in OSCAR
Energy range in MAGNEX	20.8 - 34.0 MeV for ^{4}He
Energy range in OSCAR	2.5 - 9.0 MeV for ^{3}H
	5.0 - 11.2 MeV for ^{3}He
MAGNEX angular range	$1.5^o \leq \theta_{lab} \leq 12.0^o$
OSCAR angular range	$19.0^o \leq \theta_{lab} \leq 38.0^o$

- the theoretical description of the elastic and inelastic scattering process within a coupled channel quantum scattering theory framework. Into this context, the differential cross section angular distribution data will be compared with the theoretical ones.

Last but not least, we aim to provide strong constraints to the existing theories, contributing to the solution of a puzzle which can be linked to deficiencies of our knowledge of the nuclear Hamiltonian [10].

4 Summary

The ^{4}He+^{4}He inelastic scattering was experimentally investigated at the MAGNEX facility of INFN - LNS, aiming at characterizing the 0_2^+ resonant state of ^{4}He. Thanks to an exclusive measurement, the ^{4}He+^{4}He→^{4}He+^{4}He*→^{4}He+^{3}H+p and ^{4}He+^{4}He→^{4}He+^{4}He*→^{4}He+^{3}He+n configurations were measured above the proton and neutron separation threshold energies, respectively, in an almost background free measurement. The results will be also considered together with an elastic scattering data set, measured at the same experiment, in a global theoretical interpretation.

References

[1] R. Frosch, R. E. Rand, M. R. Yearian et al., Inelastic electron scattering from the alpha particle. Physics Letters **19**, 155 (1965). https://doi.org/10.1016/0031-9163(65)90756-0

[2] R. Frosch, R. E. Rand, H. Crannell et al., Inelastic electron scattering from ^{4}He. Nuclear Physics A **110**, 657 (1968). https://doi.org/10.1016/0375-9474(68)90379-5

[3] Th. Walcher, Excitation of ^{4}He by inelastic electron scattering at low momentum transfer. Physics Letters **B31**, 442 (1970). https://doi.org/10.1016/0370-2693(70)90148-6

[4] G. Köbschall, C. Ottermann, K. Maurer et al., Excitation of the quasi-bound state in ^{4}He by electron scattering at medium momentum transfer. Nuclear Physics A **405**, 648 (1983). https://doi.org/10.1016/0375-9474(83)90523-7

[5] S. Kegel , P. Achenbach , S. Bacca et al., Measurement of the α-Particle Monopole Transition Form Factor Challenges Theory: A Low-Energy Puzzle for Nuclear Forces ?. Phys. Rev. Lett. **130**, 152502 (2023). https://doi.org/10.1103/PhysRevLett.130.152502

[6] L. E. Williams, Continuum Resonances in He$^4(p, p')$He^{4*}. Physical Review **144**, 815 (1966). https://doi.org/10.1103/PhysRev.144.815

[7] E. E. Gross, E. V. Hungerford, J. J. Malanify, J. W. Watson, Investigation of the Reaction ^{4}He (^{4}He, ^{4}He) ^{4}He* at 64 MeV. Physical Review **178**, 1584 (1969). https://doi.org/10.1103/PhysRev.178.1584

[8] M. Baumgartner, H. P. Gubler, M. Heller, The $\alpha*$ and the neutron scattering lengths of ^{3}He. Nuclear Physics A **368**, 189 (1981). https://doi.org/10.1016/0375-9474(81)90681-3

[9] E. Epelbaum, Probing the Helium Nucleus beyond the Ground State. Physics **16**, 58 (2023). https://physics.aps.org/articles/v16/58

[10] S. Bacca, N. Barnea, W. Leidemann, G. Orlandini, Isoscalar Monopole Resonance of the Alpha Particle: A Prism to Nuclear Hamiltonians. Phys. Rev. Lett. **110**, 042503 (2013). https://doi.org/10.1103/PhysRevLett.110.042503

[11] U.-G. Meißner, S. Shen, S. Elhatisari, D. Lee, Ab Initio Calculation of the Alpha-Particle Monopole Transition Form Factor. Phys. Rev. Lett. **132**, 062501 (2024). https://doi.org/10.1103/PhysRevLett.132.062501

[12] M. Kamimura, Derivation of transition density from the observed ^{4}He(e, e')^{4}He(0_2^+) form factor raising the α-particle monopole puzzle. Progress of Theoretical and Experimental Physics **2023**, 071D01 (2023). https://doi.org/10.1093/ptep/ptad090

[13] F. Cappuzzello, C. Agodi, D. Carbone, M. Cavallaro, The MAGNEX spectrometer: Results and perspectives. Eur. Phys. J. A **52**, 167 (2016). https://doi.org/10.1140/epja/i2016-16167-1

[14] D. Dell'Aquila, I. Lombardo, G. Verde et al., OSCAR: A new modular device for the identification and correlation of low energy particles. Nuclear Instruments and Methods in Physics Research Section A **877**, 227 (2018). https://doi.org/10.1016/j.nima.2017.09.046

[15] V. Soukeras, F. Cappuzzello, M. Cavallaro et al., Study of the ^{4}He(^{4}He,^{4}He)^{4}He* inelastic scattering at the MAGNEX facility. EPJ Web of Conferences **252**, 04007 (2021). https://doi.org/10.1051/epjconf/202125204007

[16] V. Soukeras, F. Cappuzzello, C. Agodi et al., Revisiting the ^{4}He(^{4}He,^{4}He)^{4}He* inelastic scattering at the MAGNEX facility. Journal of Physics: Conference Series **2586**, 012033 (2023). https://doi.org/10.1088/1742-6596/2586/1/012033

[17] M. Cavallaro, F. Cappuzzello, D. Carbone et al., The low-pressure focal plane detector of the MAGNEX spectrometer. Eur. Phys. J. A **48**, 59 (2012). https://doi.org/10.1140/epja/i2012-12059-8

[18] D. Carbone, F. Cappuzzello, M. Cavallaro, Universal algorithm for the analysis of charge distributions in segmented electrodes of gas detectors. Eur. Phys. J. A **48**, 60 (2012). https://doi.org/10.1140/epja/i2012-12060-3

[19] D. Torresi, O. Sgouros, V. Soukeras et al., An upgraded focal plane detector for the MAGNEX spectrometer. Nuclear Instruments and Methods in Physics Research Section A **989**, 164918 (2021). https://doi.org/10.1016/j.nima.2020.164918

[20] F. Cappuzzello, M. Cavallaro, A. Cunsolo et al., A particle identification technique for large acceptance spectrometers. Nuclear Instruments and Methods in Physics Research Section A **621**, 419 (2010). http://dx.doi.org/10.1016/j.nima.2010.05.027

[21] F. Cappuzzello, D. Carbone, M. Cavallaro, Measuring the ions momentum vector with a large acceptance magnetic spectrometer. Nuclear Instruments and Methods in Physics Research Section A **638**, 74 (2011). https://doi.org/10.1016/j.nima.2011.02.045

[22] A. Lazzaro, F. Cappuzzello, A. Cunsolo et al., Field measurement for large quadrupole magnets. Nuclear Instruments and Methods in Physics Research Section A **591**, 394 (2008). https://doi.org/10.1016/j.nima.2008.02.103

[23] A. Lazzaro, F. Cappuzzello, A. Cunsolo et al., Field measurement for large bending magnets. Nuclear Instruments and Methods in Physics Research Section A **585**, 136 (2008). https://doi.org/10.1016/j.nima.2007.10.046

[24] O. Sgouros, V. Soukeras, A. Pakou, Multip : A Multi Purpose simulation Monte Carlo algorithm for two- and three-body reaction kinematics. Eur. Phys. J. A **53**, 165 (2017). https://doi.org/10.1140/epja/i2017-12359-5